C-band Dual-Polarization Radar Observations of a Massive Volcanic Eruption in South America

Luciano Vidal, Stephen W. Nesbitt, Paola Salio, Camila Farias, María Gabriela Nicora, María Soledad Osores, Luigi Mereu, and Frank S. Marzano, *Fellow, IEEE*

***Abstract*—The eruption of Calbuco volcano on April 22–23, 2015 is the first volcanic eruption detected by a weather radar in South America. The detection was performed by the first domestically produced Argentinean weather radar, called RMA0 and located at Bariloche International Airport. It is a C-band Doppler dual-polarization system, manufactured by INVAP S.E. as a part of the new radar network of Argentina. The aim of this study is to present analysis of the time evolution of the structure of the volcanic plume using polarimetric observables. In order to explore the potential of this new data set for the analysis of the Calbuco volcano eruption column and dispersed ash cloud, synthetic backscattering signatures at C-band have been simulated and used to set up a threshold-based algorithm for tephra-type classification. An evaluation of lightning activity and its relationships with the volcanic particle spatial distribution and attendant polarimetric radar signatures are also discussed.**

***Index Terms*—Calbuco volcano, C-band meteorological radar, lightning activity, polarimetric signatures, volcanic ash.**

I. Introduction

THE Volcanic ash dispersed in the atmosphere after eruptions has a large impact on the environment, climate, and society, and presents many hazards [1]. The monitoring of a volcano eruption in real time, in terms of its intensity and plume characteristics, is not always possible by conventional visual inspections. Remote sensing techniques both from ground and space represent unique tools to be exploited [2]. In particular, microwave weather radars can gather 4-D information of atmospheric ash-cloud scattering volumes up to several hundreds of kilometers, in all weather conditions, at a fairly high spatial resolution (less than a kilometer) and with a repetition cycle of few minutes.

When the observation is close to the volcano vent, remote sensing instruments can be used to estimate the near-source eruption characteristics. The most important near-source parameters are the plume height and mass eruption rate [3]–[7]. The retrieval of these parameters represents an important input for ash dispersion models, which are used to predict the geographical areas likely to be affected by ash [8]. Tephra is usually referred to materials of all types and sizes, erupting from a crater or volcanic vent as a result of an intensive magma and rock fragmentation [9]. Tephra is characterized by typical diameter, residence period in the atmosphere, and the distance from the vent that volcano debris can reach [10], [11]. Ash is very fine-grained fragments (<2 mm) and is generally dominated by broken glass shards, but with variable amounts of broken crystal and lithic (rock) fragments. Lapilli may look like cylinders, and within water-rich eruptions, the accretion of wet ash may form rounded spheres known as accretionary lapilli. Larger erupted materials, like bombs, have shapes or textures such as vesicularity that indicate they were liquid or plastic when erupted. Blocks, generally, are more angular and solid when erupted [12].

Several volcanic eruptions worldwide have been observed by ground-based weather radars, even though most of these observations were performed by single polarization radars. The Mount St. Helens (USA) volcanic activity in 1980–1982 was the first eruption documented using the U.S. National Weather Service radar system at C-band in Portland [13]. In [14], Lacasse *et al*. studied the volcanic cloud related to the Hekla eruption in Iceland on November 2000, and it was the first eruption to be continuously and completely monitored. The eruption plume, mainly coarse ash particles, reached a height of 6–10 km relative to the Hakla vent, as clearly detected by the Keflavik operational C-band single-polarization radar located in southern Iceland [15], [16]. The latter radar clearly detected the explosive eruption plume, mainly due to coarse ash particles, of the Grímsvötn volcano in Iceland on November 2004 [15], [16]. The

Manuscript received March 8, 2016; revised July 1, 2016, September 19, 2016, and November 10, 2016; accepted December 7, 2016. This work was supported by ANPCyT PICT 2013-1299, UBACyT 2013-2016-20020130100618BA, PID-DEF 05/14, ALERT.AR Cooperation Project, and the European Union's Seventh Framework Programme (FP7/2007-2013) through the Project APhoRISM under Grant 606738. *(Corresponding author: Luciano Vidal.)*

L. Vidal is with the Servicio Meteorológico Nacional, Buenos Aires C1425GBE, Argentina (e-mail: lvidal@smn.gov.ar).

S. W. Nesbitt is with the Department of Atmospheric Sciences, University of Illinois, Urbana-Champaign, IL 61801 USA (e-mail: snesbitt@illinois.edu).

P. Salio is with the Centro de Investigaciones del Mar y la Atmósfera, Departamento de Ciencias de la Atmósfera y los Océanos, Universidad de Buenos Aires—CONICET, Buenos Aires C1425GBE, Argentina, and also with UMI-IFAECI CNRS 3351, Buenos Aires C1425GBE, Argentina (e-mail: salio@cima.fcen.uba.ar).

C. Farias is with the Servicio Meteorológico Nacional, Buenos Aires C1425GBE, Argentina (e-mail: cfarias@smn.gov.ar).

M. G. Nicora is with CEILAP-UNIDEF (Ministerio de Defensa/CONICET), Villa Martelli Argentina, and also with UMI-IFAECI CNRS 3351, Buenos Aires C1425GBE, Argentina (e-mail: gnicora@citedef.gob.ar).

M. S. Osores is with the Servicio Meteorológico Nacional, Buenos Aires C1425GBE, Argentina, and also with CONICET/CONAE, Buenos Aires C1425GBE, Argentina (e-mail: msosores@smn.gov.ar).

L. Mereu and F. S. Marzano are with the Dipartimento di Ingegneria dell'Informazione, Elettronica e Telecomunicazioni Sapienza Università di Roma, Rome 00184, Italy (e-mail: luigi.mereu@diet.uniroma1.it; marzano@diet.uniroma1.it).

Color versions of one or more of the figures in this paper are available online at http://ieeexplore.ieee.org.

Digital Object Identifier 10.1109/JSTARS.2016.2640227

signal of volcanic cloud was quite evident from the range-height indicator radar reflectivity scans, with radar reflectivity values observed up to 20 dBZ. The plume top altitude was about 15 km, although this number may depend on the radar sensitivity and beam characteristics. Evidence of a volcanic plume, measured by S-band weather radar of Guadeloupe during the Soufriere Hill volcano eruption, was observed on March 20, 2000 [17]. Another massive eruption, observed by a single polarization radar, was the Augustine volcano eruption in Alaska, occurred around 13:00 UTC on January 13, 2006. It was observed by the S-band weather radar operated by the U.S. Geological Survey (USGS) Alaska Volcano Observatory. The PPI image sequence clearly shows the possibility to detect the spatial and temporal evolutions of the ash plume using this sensor [18].

Dual-polarization technology produces additional data providing valuable information on the shape and nature of the detected particles. These variables can be considered to better estimate particle concentration and the size of the column eruption together with ash volume, ash fall, and total mass. The first eruption documented by a dual-polarization radar worldwide was the Etna eruption that occurred on April 10, 2011 and it volcanic ash cloud was clearly observed by the mobile polarimetric X-band radar, located inside the Catania airport [5]. Maki *et al.* [7] analyzed operational C-band dual polarization weather radar data from 27 large eruptions of the Mt. Shinmoedake volcano in the Kirishima range in Kyushu, Japan, during the period from January to March 2011 to examine the possibility of using radar for quantitative volcanic ash estimation. The eruption time period, maximum and accumulated horizontally polarized reflectivity factor (Z_{HH}), and differential reflectivity (Z_{DR}) were observed for each eruption. More recently, the 2011 eruption of the Grímsvötn volcano, located in Iceland, was studied by Montopoli *et al.* [2]. In their study, a comparison was made using a multifrequency radar characterization, X-band dual-polarization radar, C-band radar, and observations from the satellite Special Sensor Microwave Imager (SSM/I) in order to estimate the near-source volcanic ash cloud parameters. Crouch *et al.* [19] recently presented a description of the first volcanic eruption observed by an operational weather radar in New Zealand. The Mt. Tongariro Upper Te Maaru Crater had an eruption on August 6, 2012 which was observed by the MetService Bay of Plenty dual-polarization C-band weather radar.

There are other ground-based remote sensing sources that allow monitoring volcano activity with global coverage: lightning detection networks. Recently, research relating lightning and volcanic eruptions were performed in order to investigate the potential use of this dataset as an indicator of the volcanic activity and electrification processes in volcanic clouds [20]–[24]. In [25], McNutt and Williams showed a correlation between the Volcanic Explosivity Index (VEI) and the number of volcanic eruptions with lightning activity. Results are coherent with the hypothesis of big eruptions (associated with VEI between 3 and 6) where the volcanic plume is characterized by strong vertical development, similar to deep moist convection. In [26], the lightning activity in South America associated with the Cordon Caulle eruption during June 2011 using the Word Wide Lightning Location Network (WWLLN) was studied. The observed electrical activity is consistent spatially and temporally with the time evolution of volcanic plume. The location of highest lightning activity was detected in a southeasterly direction from the volcano, consistent with the prevailing direction of the wind and the observed plume (although the electrical activity detected was relatively low and limited to the plume itself). Recently, in [27], an analysis of the volcanic lighting and plume behavior during the Calbuco eruption in April 2015 was presented. Van Eaton *et al.* [27] demonstrated that changes in the lightning activity and satellite-detected plume dynamics may be used to infer key aspects of eruption behavior, including the mass eruption rate, volume, start time, and duration.

Although there are prior studies of the time evolution of the erupted volcanic plume using remote sensing instrumentation, this paper is focused on four main goals:

1) to provide the first case study analysis of weather radar observations of a sub-Plinian volcanic plume in South America through the analysis of the Calbuco volcanic eruption in 2015;
2) to interpret model-based dual-polarization radar signatures of ash particle volumes in terms of statistical properties at C-band as an extension of what already carried out at X-band;
3) to create an objective ash classification using a C-band dual-polarized Doppler weather radar data and discussing the sub-Plinian explosive eruption processes; and
4) to evaluate the combined availability of lightning data as an indicator of the Calbuco volcanic eruption intensity and its main properties.

This paper is organized as follows. In Section II, we give a description of the characteristics of the Calbuco volcano and its last eruptions, together with a description of the dual-polarization radar system and lightning data used in this work. Polarimetric backscattering response at C-band is simulated and analyzed in terms of its signature and correlation with ash concentration in Section III using a radar scattering response microphysically based model. A description of the Calbuco eruption second pulse, using radar images in conical and cross-sectional sectors and an interpretation of volcanic particles classification algorithm are presented in Section IV. A correlation analysis among lightning activity, volcanic particle distribution, and polarimetric signatures is described in Section V. Finally, concluding remarks are discussed in Section VI.

II. Calbuco Volcano Eruption and Available Data

Calbuco is a stratovolcano located in southern Chile at 41°19'33.6"S – 72°36'50.4"W (see Fig. 1) with an altitude of 2003 m above mean sea level (AMSL). It has had 36 confirmed eruptions in its history, with 13 eruptions recorded since 1893. The last most important eruption was in 1961. Calbuco is a very explosive andesite volcano whose lavas usually contain 55% to 70% of SiO_2 (silicon dioxide), this level determines an intermediate level of acidity. The more acidic is the concentration, more explosive is the eruption giving evidence of greater height of eruptive column.

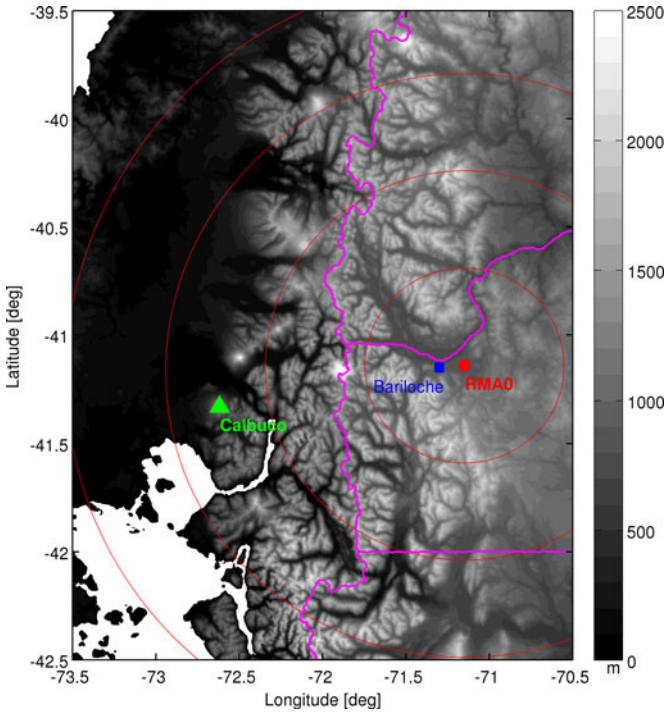

Fig. 1. Location of Calbuco volcano (triangle), and the RMA0 weather radar site (red dot). The digital elevation model in meters, sampled into the polar coordinates radar references system, is shown in shaded. Distance between rings is 50 km.

According to its evolution, geochemistry and historical eruptive activity, Calbuco is considered to be one of the most hazardous active volcanoes in the Chilean Andes [28]–[31]. It is elongated in a SW-NE direction and is capped by a 400–500-m wide summit crater. Its complex evolution included the collapse of an intermediate edifice during the late Pleistocene that produced a debris avalanche.

A. *Explosive Eruption on April 2015*

In the evening on April 22, 2015 at 21:04 UTC, Calbuco volcano had the first eruption after more than 50 years of being dormant, producing an eruptive column that reached 16 km in a few minutes, information provided by National Service of Geology and Mineralogy of Chile (Servicio Nacional de Geología y Minería de Chile, SERNAGEOMIN). According to a special report of volcanic activity issued by SERNAGEOMIN, this event was preceded by an increase in seismic activity associated with the volcano area, which began about an hour before the first eruption, on the eastern flank of the main vent. After this episode (20:35 UTC), the region began to experience record earthquakes associated with flows inside the volcano. Note that the seismic activity in the area has been insignificant since 2009 when seismic monitoring began in real time by the Southern Andes Volcanologist Observatory. After a large seismic event (2054 UTC), vigorous eruptive column reached a height greater than 15 km above the main vent. The pyroclastic dispersal was observed to be mainly to the E-NE of the volcano. The most energetic phase lasted over 1.5 h.

TABLE I
SPECIFICATIONS OF THE RMA0 WEATHER RADAR SYSTEM IN BARILOCHE (ARGENTINA)

Type	C-band INVAP S.E. radar system (5.6 GHz)
Operation since	December 2014
Location	41°08'23"S, 71°08'59"W
Height of antenna	778 m AMSL
Peak transmitted power	350 kW
Pulse duration	3.2 μs
Wavelength	5.6 cm
Pulse repetition time	2000 μs
Maximum range	300 km
Range Bin Spacing	0.48 km
Beam Width	0.98/0.98 degrees
Beam Elevations	12 elevations from 0.5 to 15.1 degrees
Task CycleTime	9 min
Recorded Fields	Horizontal Reflectivity (Z_{HH}), Vertical Reflectivity (Z_{VV}), Radial Velocity (V), Spectral Width (W), Correlation Coefficient (ρ_{HV}), and Differential Phase Shift (Φ_{DP}).
Distance from Calbuco Volcano	124 km

Seven hours after the first eruption, a massive second explosion occurred on April 23, 2015 at 04:00 UTC, producing an ash cloud with an estimated height of 20 km that penetrated the tropopause, and injected a lot of ash into the stratosphere. This higher energy phase lasted 6 h. The eruption column was dispersed into the N, NE, and E. This event, especially during its initial phase, was accompanied by a continuous emission of fragments of incandescent ballistic material, which was dispersed within 5 km of the main vent. During these two pulses, pyroclastic flows reached 8 km from the vent in the NE and SW flanks [31].

B. *Dual-Polarization Weather Radar Specifications*

The weather radar at Bariloche International Airport (41°09'04"S – 71°09'27"W) located close to the Andes range in the northwestern Patagonia region of Argentina (see Fig. 1). This radar was the first operational weather radar in South America to capture a volcanic eruption. It is a INVAP S.E. Dual Polarization C-Band Doppler prototype radar that was installed in September 2014, and called RMA0 (Radar Meteorológico Argentino 0). This prototype was built under a large project called the National System of Weather Radars (Sistema Nacional de Radares Meteorológicos, SINARAME). SINARAME is an Argentinean effort to expand the radar network over the whole country. RMA0 is located at a height of 778 m AMSL, and a distance of 124 km from Calbuco volcano oriented at 262° azimuth. The weather radar monitors precipitation and precipitating clouds within a maximum range of 300 km from its location. The description and specifications of the radar system are given in Table I.

The scanning strategy for normal weather monitoring made 300 km volume scans for 12 elevations as well as 120-km Doppler scans for nine elevations, both every 9 min. The representation of the beam propagation in a range-height reference system is shown in Fig. 2. The beam height was calculated utilizing a standard atmospheric refraction model [32], using the

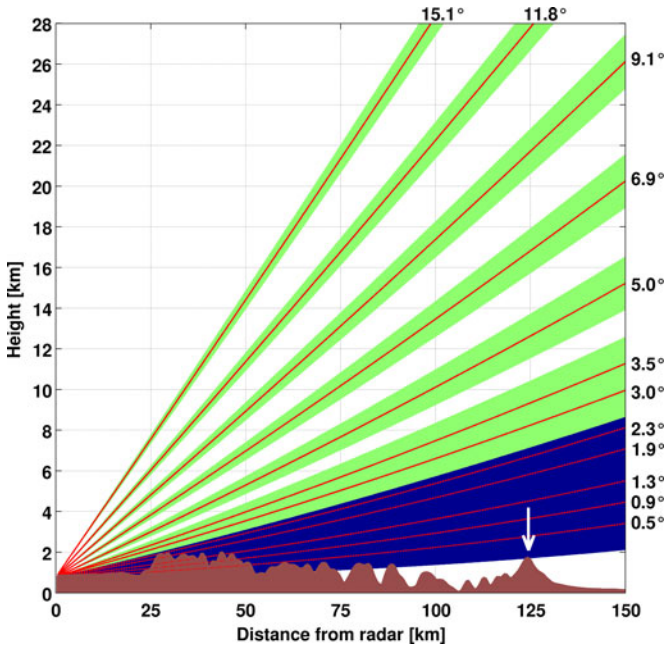

Fig. 2. RMA0 radar scanning strategy during Calbuco volcano eruption in April 2015. The antenna elevation angles (degrees) are shown close to each theoretical radar ray paths for a standard atmosphere with red lines; green shaded areas indicate the 1° radar beamwidth. Antenna elevations totally blocked by the topography are indicated by dashed lines, blue shaded areas indicate 1° radar beamwidth associated with blocked rays. The terrain elevation profile along the direction of 262° is also displayed in brown. The radar is positioned at the origin of the axes, and the Calbuco volcano (arrow) is at 124 km away from the radar.

following equation:

$$H = \sqrt{r^2 + R^2 + 2 * r * R * \sin\varphi} - R \qquad (1)$$

where H is the altitude of the central radar beam above sea level (km), r is the range (km) from the radar to the point of interest, φ is the antenna elevation angle (degrees), and R is 4/3 the radius of the Earth. Note that the first four tilts (up to 1.9° antenna elevation) are blocked by topography in the direction of the Calbuco volcano, and the fifth tilt (2.3°) is partially blocked for a standard atmosphere. Under these modeled conditions, the lowest elevation angle of the beam reaching Calbuco used is 3° for the purpose of this paper, which is 8.2 km AMSL) at the range of the volcano (∼6 km above volcano crater). The down-range distance from the radar to Calbuco was 124 km, producing central beam heights from 8.2 to 21.4 km above sea level for scan elevation between 3° and 9.1° shown in Fig. 2.

C. Lightning Data

Data from the WWLLN [33] were used to analyze the eruption dynamic in combination with radar observations. WWLLN is a global lightning network that detects the very low frequency (VLF; 3–30 kHz) emissions from lightning, known as spherics, that propagate long distances through the Earth-ionosphere waveguide. The WWLLN, a research collaboration led by the University of Washington, USA, is an expanding, global network currently composed of ∼55 sensors with an increasing detection efficiency (20–40% for high amplitude strokes), location accuracy (<9 km), and detections available within 1 min. This network uses the time of group arrival technique to detect spheric waveforms for lightning location within ∼5 km and <10 μs [34]. WWLLN preferentially detects intense cloud-to-ground (CG) lightning [35], [36] and the network cannot provide a discrimination between CG and intracloud lightning. In this study, lightning data have been grouped into time windows of 9 min focusing on radar data time.

III. Polarimetric Weather Radar Data Interpretation at C-Band

The polarimetric variables, obtained from RMA0 weather radar used in this paper, are Z_{HH} and vertical radar reflectivity factor (Z_{VV}), both in dBZ, the correlation coefficient (ρ_{HV}), and the differential phase shift (K_{DP}, °/km) with range and azimuth resolutions of 0.48 km and 1°, respectively. A qualitative description of these observables is briefly provided followed by the analysis of synthetic signatures, generated by a backscattering model valid at C-band.

A. Polarimetric Radar Observables

The Z_{DR} is not an output variable from the radar processor, but it was calculated from Z_{HH} and Z_{VV}. A Z_{DR} offset value was considered as –4.6 dB provided by INVAP S.E. through a vertical pointing scanning, and considered in Z_{DR} calculation. Values of Z_{HH} are proportional to the size and number concentration of particles within the radar resolution volume. However, larger ash particles tend to provide a much larger contribution to Z_{HH} than smaller particles of equal abundance [19], [37], [38]. Z_{DR} is a good indicator of the mean size and shape of the particles within the sampling volume. Values of Z_{DR} close to zero indicate spherical particles (e.g., small hail and drizzle or tumbling large hail for meteorological targets or randomly oriented oblate/prolate ash particles), whereas positive and negative values indicate horizontally (e.g., rain, melting hail for meteorological targets) and vertically oriented particles (e.g., ice crystals aligned vertically by a thunderstorm's electric field), respectively. The discrimination between spherical and nonspherical fine and coarse ash particles has a particular interest due to different settling particles velocity [39]. The typical dynamical range of Z_{DR} in a meteorological echo is between -5 and 8 dB, but, for ash, simulations indicate that values larger than 3 dB are unlikely to occur [2].

The correlation coefficient, ρ_{HV}, measures the phase consistency of the returned signal in the H and V polarizations in terms of signal power and phase for each received pulse [2]. This correlation helps us to understand information about the diversity (e.g., size, shape, orientation, and mixture) of targets within the sampled radar volume and is a value which ranges between 0 and 1. On the other hand, it is hypothesized that high ρ_{HV} (>0.97) indicates that the ash particles within the radar sampling volumes are very uniform in size, shape, and orientation, and, as a consequence, indicates negligible turbulence effects. Values close to unity (0.96 to 1) generally indicate small diversity in the targets (e.g., the sample volume consists of only raindrops, ice particles, or similar sized and shaped ash particles). Values ranging from 0.85 and 0.95 indicate a diversity

in the targets within the radar resolution volume (e.g., mix of rain and ice particles, or possible a mix of different sized and shaped ash and lapilli particles). Values less than 0.85 are usually associated with nonmeteorological targets or with a diverse mixture of different particles within the same radar sampling volume (e.g., mix of water droplets, ice crystals, ash, lapilli, and larger ballistics). For ash, low ρ_{HV} (i.e., lower than 0.80) is hypothesized to imply a large degree of diversity within the radar sampling volume.

A further interesting polarimetric observable is the K_{DP} which is due to the forward propagation phase difference between the two polarizations and can be derived from the measured two-way differential phase shift. The information carried by K_{DP} is similar to that of ρ_{HV}, even though related to forward scattering [12].

B. Simulating Volcanic Particle Polarimetric Backscattering at C-Band

The interpretation and evaluation of the geophysical information from polarimetric radar observations during volcano activity is not an easy task, especially limited to the few available experimental analyses [11]. To derive quantitative results from the radar data, we have used synthetic data set of radar observables generated by a physical-electromagnetic forward model extended from X-band to C-band [12]. The extension has been simply carried out by setting the wavelength from X to C band. This is possible via the HAPESS forward model, based on T-matrix scattering solution. The refractive index model are valid at least up to Ka-band (35 GHz) thus including both C- and X-band. C-band simulations of radar variables for tephra particles is something not covered in past publications and represent a novel contribution to the study of volcanic cloud from weather radars.

The simulation of radar variables are performed making the hypothesis that only tephra is composing the particles within the volcanic column, and no mixture or aggregates are considered. A previous work [18] aimed at quantifying the possible impact of mixtures and/or aggregates of ash and liquid/ice particles on radar reflectivity measurements. However, apart from the zero thermal altitude estimation, dual-polarization radars are not able to discriminate pure tephra from tephra/hydrometeor aggregate. This means that, even though we can simulate ash/hydrometeor aggregates, we cannot train our inversion algorithms to discriminate between pure ash and ash/hydrometeor aggregates. Moreover, there are a lot of uncertainties in the forward modeling of ash/hydrometeor aggregates due to the unknown shape, orientation, and composition. In conclusion, at the stage of current knowledge, a more conservative approach is to increase the noise contribution in our inversion procedures and live with a larger interval of variability of our estimates [15].

Synthetic data are obtained by letting the ash particle size distribution parameters and the particle orientation, supposed to be spheroids, to vary in random way. Additional information, like ash particle density, axis ratio, and dielectric constant are assumed *a priori*. More details about the radar response model and its rationale are available in [12]. A microphysical model of volcanic clouds for radar observation is proposed in terms of four main classes (or modes) of ash size: fine ash (FA), coarse ash (CA), small lapilli (SL), and large lapilli (LL). To simulate a wide variety of observation conditions, within each class, a random distribution can be assumed for, including 1) average particle diameters (e.g., equal to 0.01, 0.1, and 1 mm for fine, coarse, and lapilli, respectively); 2) average ash concentration (C_a) with a mean value equal to 0.1, 1, and 5 $\mathrm{g\,m^{-3}}$ for light, moderate, and intense concentration regimes, respectively; and 3) angular average orientation labeled as prolate (PO: when the particle major axis, assumed to have a spheroidal shape, is vertical with respect to the surface), oblate (OO: when the predominant major axis is horizontal), and tumbling (TO: when there is not any predominant orientation).

This section is devoted to the illustration of the ash subclass signatures in terms of polarimetric observables simulated with the aim of understanding which measurement variability may be expected at C-band. The correlograms among the radar polarimetric observables are sometimes called "self-consistency" plots [11], [12]. Indeed, this analysis is aimed at: 1) identifying the ash classes which can be actually discriminated with the available measurements and 2) evaluating the cross correlation among the radar observables in order to perform a powerful quality check of the measurements once acquired and processed by the radar system. We will order this analysis in the following text by size classes under the assumption of rhyolitic axis ratio.

The first analysis refers to the coarse ash class (CA) in Fig. 3(a)–(c) whose analysis corroborates the following considerations: 1) Z_{DR} clearly distinguishes among OO, PO, and TO; 2) ρ_{HV} may help to discriminate among PO, OO, and TO subclasses; 3) K_{DP} is sensitive to both OO and PO.

The second analysis refers to the SL class in Fig. 3(d)–(f), providing comments similar to those for the CA class: 1) Z_{DR} clearly distinguishes among OO, PO, and TO; 2) the signature of ρ_{HV} may help to discriminate among the PO and OO (the latter overlaps with TO) subclasses when compared with Z_{DR}; 3) K_{DP} is sensitive to both OO and PO.

The third analysis refers to the LL class in Fig. 3(g)–(i). Some further considerations, to be compared with those of the other ash classes, are summarized as: 1) Z_{DR} helps us to distinguish among OO, PO, and TO, but in a way less straightforward than those for other size classes. The TO class is fairly confused with the PO class. 2) the signature of ρ_{HV} does not help to discriminate among the PO and TO subclasses; 3) K_{DP} does not help to discriminate among OO and PO, compared with smaller size classes.

Fig. 3 also highlights the expected statistical variability of the polarimetric radar observables due to ash polydispersions. In this respect, it is worth noting the following features:

1) CA see Fig. 3(a)–(c) can cause values of Z_{HH} as low as –15 dBZ for very small ash concentrations and up to 30 dBZ for large concentrations, whereas values of Z_{DR} may be between –0.2 and 0.2 dB for TO fall ash, while less than –0.3 dB (down to –1.5 dB) for PO particles and larger than 1 dB (up to 2 dB) for OO particles. For tumbling fall ash, K_{DP} shows a very low dispersion ranging between –0.5° and +0.55 °/km, a correlation coefficient ρ_{HV} between

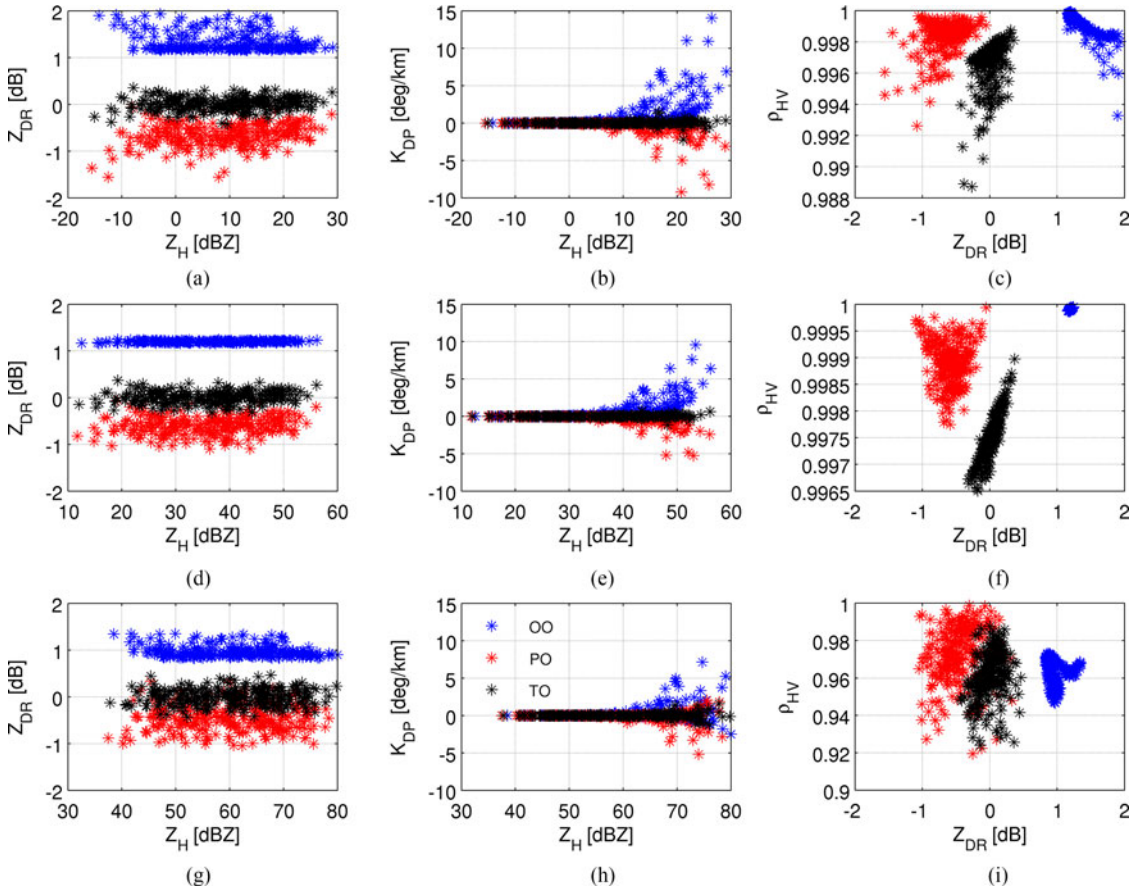

Fig. 3. Correlation between main C-band radar observables ($Z_{\rm HH}$, $Z_{\rm DR}$, $K_{\rm DP}$, and $\rho_{\rm HV}$); see text for their definitions) for CA (upper), SL (center), and LL (bottom) size classes, UC concentration and different particle orientations (PO, TO, and OO) under the assumption of rhyolitic axis ratio.

0.992 and 0.999, whereas for PO fall ash, $K_{\rm DP}$ is within 0 and –10 °/km, and high correlation coefficient $\rho_{\rm HV}$ (larger than 0.998). For oblate fall ash, $K_{\rm DP}$ is within 0 and 15 °/km with correlation coefficient $\rho_{\rm HV}$ between 0.994 and 1.

2) SL see Fig. 3(d)–(f) are associated with values of $Z_{\rm HH}$ between 10 and 55 dBZ, going from small ash concentrations (10^{-3} g/m^3) to intense concentrations (10 g/m^3), whereas values of $Z_{\rm DR}$ may be between –0.4 and 0.3 dB for TO fall ash, while less than –0.4 dB (down to –1.1 dB) for PO particles and a mean value of 1.25 dB for OO particles with a very low dispersion. For TO fall ash, $K_{\rm DP}$ is limited within –0.5°/km and +0.5°/km with a correlation $\rho_{\rm HV}$ between 0.996 and 0.999, whereas for prolate fall ash, $K_{\rm DP}$ is within 0°/km and –5°/km with correlation coefficient $\rho_{\rm HV}$ between 0.998 and 0.999. For oblate fall ash, $K_{\rm DP}$ is within 0 and 10°/km, with a high correlation $\rho_{\rm HV}$ (close to 1).

3) LL see Fig. 3(g)–(i) give values of $Z_{\rm HH}$ between 40 and 80 dBZ, going from small ash concentrations to intense concentrations, whereas values of $Z_{\rm DR}$ may be between –0.4 and 0.4 dB for tumbling fall ash, while less than 0.2 dB (down to –1 dB) for oblate particles. This behavior, different from CA and SL, may be explained by invoking the Mie effects. For TO fall ash, $K_{\rm DP}$ is limited within –2°/km and +2°/km, with a correlation coefficient $\rho_{\rm HV}$ between 0.92 and 0.98, whereas for PO fall ash, $K_{\rm DP}$ is within –6 and 2°/km with correlation $\rho_{\rm HV}$ between 0.92 and 1. For oblate fall ash, $K_{\rm DP}$ is within –2 and 7°/km with correlation coefficient $\rho_{\rm HV}$ between 0.94 and 0.98.

TABLE II
SCHEME OF THE SINGLE-VALUE DECISION THRESHOLDS USED IN THE VOLCANIC PARTICLE CLASSIFICATION ALGORITHM

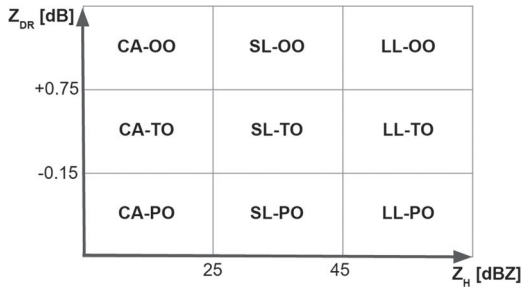

This backscattering simulation allows us to propose an volcanic particles class identification model for C-band polarimetric radar data considering two inputs as a first approximation, i.e., $Z_{\rm HH}$ and $Z_{\rm DR}$. This partitioning algorithm consists in a single-value decision threshold where two characteristics are distinguished volcanic particle size and falling orientation:

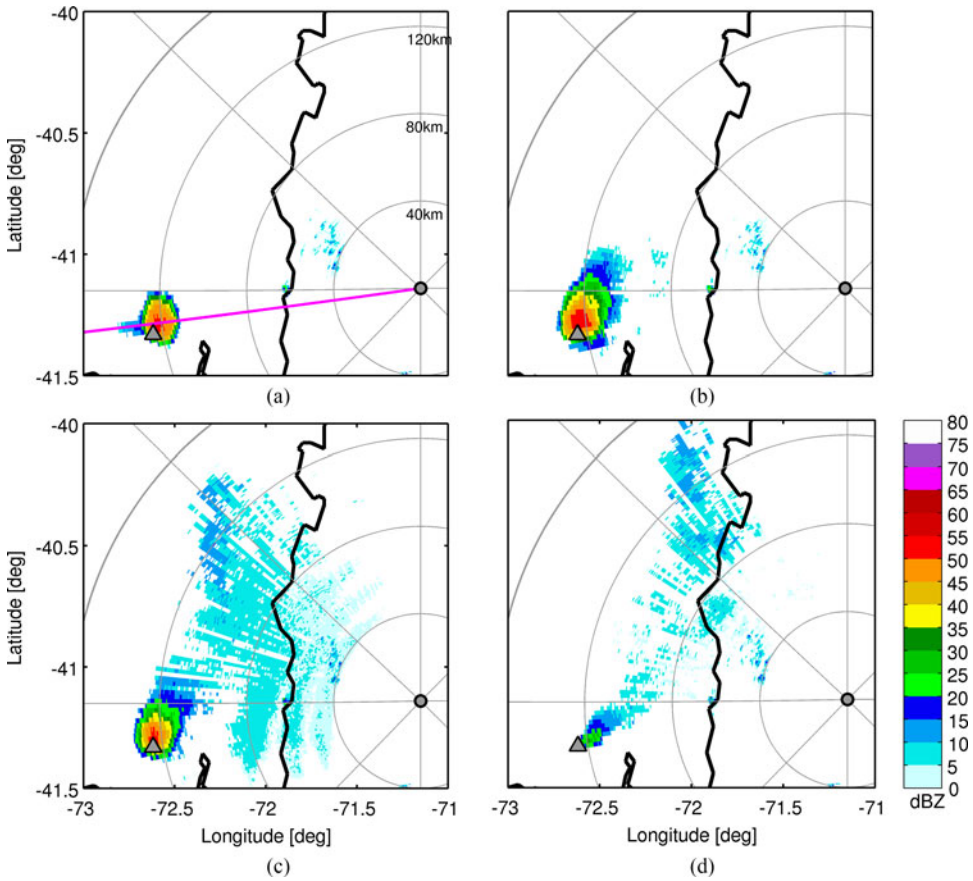

Fig. 4. Vertical maximum horizontal reflectivity for the Calbuco volcano eruption on April 23, 2015 at four different moments: (a) 04:09 UTC, (b) 04:44 UTC, (c) 07:15 UTC, and (d) 09:54 UTC. The magenta-colored line shows the azimuth at 262° where vertical cuts in Fig. 6.

1) classification of radar echoes with respect to particle size (CA, SL, and LL) based on Z_{HH} values, and 2) falling orientation (PO, OO, and TO) based in Z_{DR} values. To characterize the behavior of these particles, the backscattering simulation suggests approximate thresholds for Z_{HH} and $Z_{\mathrm{DR},}$ to distinguish between these proposed categories. Numerous scattering simulations were carried out at C-band, intended to span possible physical conditions associated with each particle type. Thresholds for both variables were obtained from the scatterplot between Z_{HH} and Z_{DR}. Fig. 3(a), (d), (g) from numerical simulations considering the mean of each variable and 1.5 sigma interval, as schematically shown in Table II.

IV. Calbuco Eruption Second Pulse From Radar Observations

The RMA0 radar detected the onset of the second massive eruption in the scan beginning at 04:00 UTC. At 04:09 UTC [see Fig. 4(a)], the vertical maximum (COLMAX) of the horizontally polarized reflectivity shows values greater than 50 dBZ can be observed associated with large targets within the main column (e.g., coarse ash, small, and large lapilli), and an echo top close to 22 km AMSL (20 km relative to the Calbuco vent). Of particular interest there is the three-body scatter spike (TBSS) echoes observed along a radial downrange from the areas of highest reflectivity in the eruption column. This signature indicates that scattered reflections from large cloud particles at higher altitudes (between 4.5 and 11.9 km above the Calbuco vent as determined from the inspection of individual radar tilts) within the eruption column toward the ground which, in its turn, scatters in the backward direction again toward the larger particles, which subsequently scatter onward to the radar antenna. This behavior is observed frequently by weather radar in thunderstorms containing large hail [40], but it was also observed in the Upper Te Maari eruption during August 6, 2012 in New Zealand [19].

At 04:44 UTC [see Fig. 4(b)], COLMAX imagery shows the coarse ash plume starting to drift downwind toward the north and northeast away from the vent. Then, 3 h later [see Fig. 4(c)], the coarse ash cloud, with horizontally polarized reflectivity values range from 5 to 15 dBZ, continued drifting downwind toward the northeast away from the volcano. Reflectivity around 10 to 15 dBZ, associated with higher concentrations of ash or larger volcanic particles, are observed in the northern part of the image. Large lapilli probably are observed associated with the main column, with reflectivity values greater than 50 dBZ. The eruption ended at 10:00 UTC; low values of COLMAX reflectivity within the vent (20–25 dBZ) and the volcanic plume well defined with a clear northeast orientation [see Fig. 4(d)].

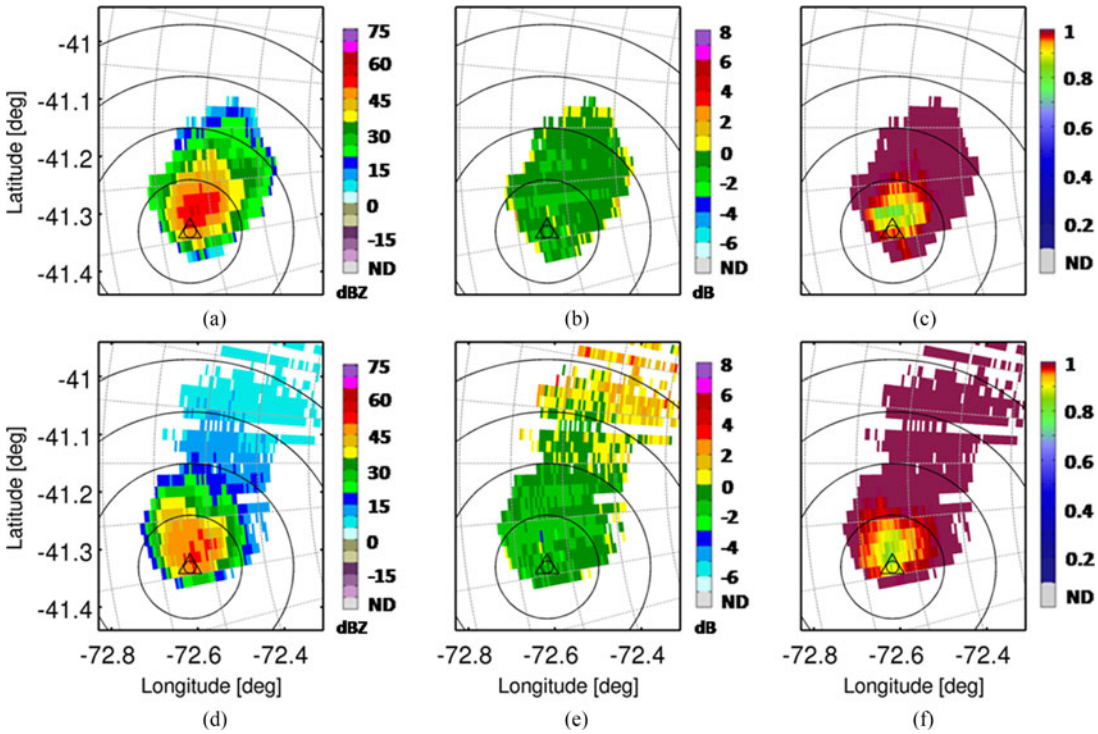

Fig. 5. Plan position indicator (PPI) at 5° of (a) Z_{HH}, (b) Z_{DR}, and (c) ρ_{HV}. April 23, 2015 at 04:18 UTC (upper panels), and 07:06 UTC (lower panels).

The volcanic cloud top shows a mean value of 22.8 $\pm$ 2.1 km AMSL (20.8 $\pm$ 2.1 km above Calbuco vent) estimated from individual PPI analysis. In spite of this, value has a strong dependency of the radar scanning strategy and the radar-volcano distance. The estimation is greater than the maximum altitude of the eruption column during the last major eruption in 1961 determined from visual telemetry close to 12–15 km. This is consistent with the results presented by Astudillo *et al.* [41], where author conclude that the Calbuco eruption was slightly more acidic than the 1961 eruption.

A. *Analysis of PPI Radar Images*

Fig. 5 shows the PPI imagery at 5° antenna elevation for two different moments during the second pulse, and polarimetric radar variables (Z_{HH}, Z_{DR}, and ρ_{HV}). The altitude of polarimetric measurements is approximately 12.5 km AMSL, or 10.5 km above Calbuco crater. Each pixel at this distance is 480 m in range and approximately 1 km wide in azimuth. At 04:18 UTC (upper panels), higher reflectivity values (>45 dBZ) are skewed over and north of the Calbuco site, influenced by the prevailing southwesterly winds on the volcanic plume. ρ_{HV} generally shows very low values between 0.75 and 0.95 associated with the vertical eruption column. This feature is due to a very large diversity of radar targets, in terms of particle size and shape. This region is well correlated with the highest portion of Z_{HH} measurements. Similar results were found by [19] during the Te Maari eruption in New Zealand. Z_{DR} is very homogeneous with a domain of negative values, likely associated with vertically orientated particles relate to the electric field as in thunderstorms.

At 07:06 UTC (bottom panels), the vertical eruption column continues to show the same pattern in the three radar variables: Z_{HH} values greater than 45 dBZ collocated with ρ_{HV} values less than 0.95, and negative Z_{DR} values. At this time, the volcanic ash cloud has spread toward the NNE. Z_{HH} values associated with the ash cloud present values between 0 and 15 dBZ, with Z_{DR} values generally positive indicating a preference for horizontally oriented ash particles falling from the cloud, and ρ_{HV} values greater than 0.95, representing a low diversity of ash particles within the cloud. As shown by Crouch *et al.* [19], ρ_{HV} values within the ongoing emission column are low to moderate (0.75 to 0.9) representing a moderate diversity of radar targets still being ejected from, or recycled above, the vent.

B. *Analysis of Radar Vertical Cross Sections*

Vertical cross sections are shown in Fig. 6 along a 262° azimuth angle in the direction of the Calbuco volcano [see Fig. 4(a)]. At 04:09 UTC, vertical cross section of reflectivity show an eruption column top of about 20 km AMSL and values greater than 50 dBZ between 8 and 12 km AMSL. The exact top of the plume is somewhat uncertain due to radar side lobes and spreading of the radar beam main lobe, which is nearly 2 km wide at the range of the plume. ρ_{HV} shows low to moderate values through most of the eruption column ranging from 0.75 at low levels to close 1 near the top, probably associated with small particles of CA and ice crystals. In [19], this behavior of ρ_{HV} is attributed to a very high diversity of targets at lower levels in the column, with increasing stratification with height, and a lower diversity of targets at the top. Z_{DR} values are generally close to zero or –1 in the column. These characteristics are associated

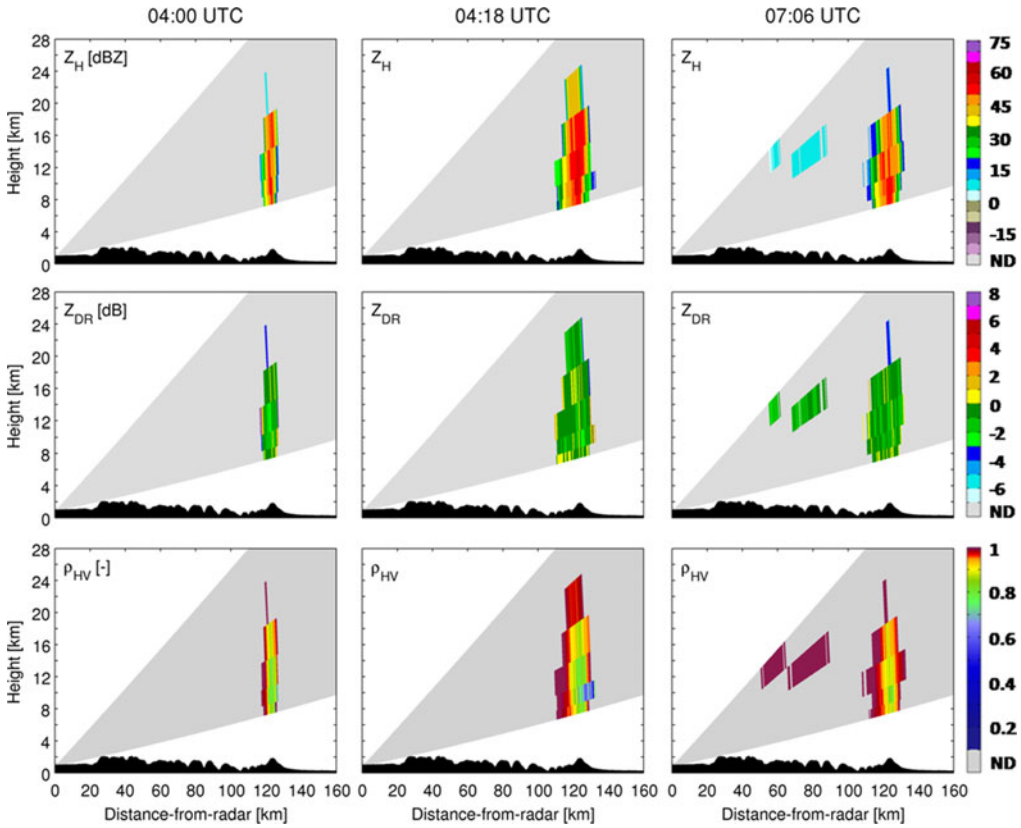

Fig. 6. Vertical cross sections of radar observables (Z_{HH}, Z_{DR}, and ρ_{HV}) along the azimuth at 262°. Left: 04:00 UTC; Center: 04:44 UTC; and Right: 07:15 UTC. The terrain elevation profile is also displayed in black.

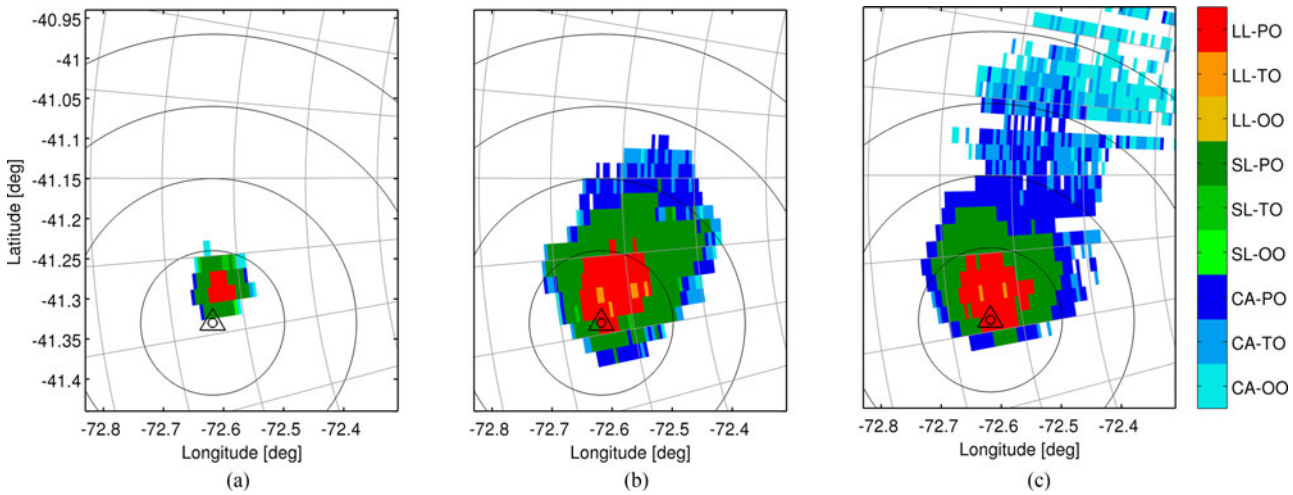

Fig. 7. Volcanic particle categories and its orientations from RMA0 radar acquisition on 23 April 2015 at (a) 04:00 UTC, (b) 04:18 UTC, and (c) 07:06 UTC. Volcanic particle categories are CA (Coarse Ash), SL (Small Lapilli), and LL (Large Lapilli). Particle orientations are OO (oblate), PO (prolate), and TO (tumbling).

with small and large vertically oriented lapilli. The TBSS region can be characterized by low values ρ_{HV} (0.25–0.65) and noisy values of Z_{DR}.

A few minutes later, at 04:44 UTC, the vertical cross section of reflectivity shows two regions with values greater than 50 dBZ, one located at 10 km and another one at 19 km AMSL. The eruption column has low to moderate ρ_{HV} values (0.7–0.85) close to the base and the moderate values (0.85–0.90) up to 24 km AMSL. Differential reflectivity values from –1 to 1 can observed, again denoting the presence of LL and CA vertically and horizontally oriented, respectively.

At 07:15 UTC, the main eruption column can be observed between 7 and 15 km AMSL, with similar structure observed as shown from earlier. Low to moderate values of ρ_{HV} ranging

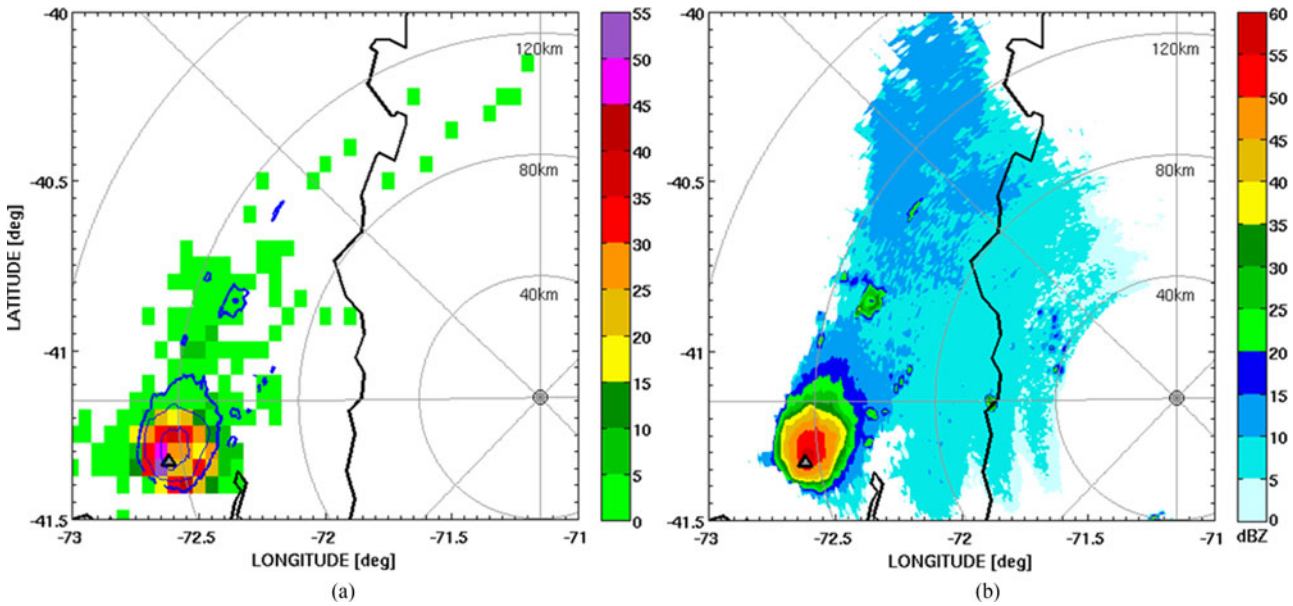

Fig. 8. (a) WWLLN total strokes for the entire second pulse of Calbuco volcano eruption. Contour of 20, 35, and 50 dBZ of COLMAX values are presented in blue color. (b) Time accumulated COLMAX between 04:00 and 11:41 UTC, April 23, 2015. The location of the Calbuco volcano is indicated by the black triangle.

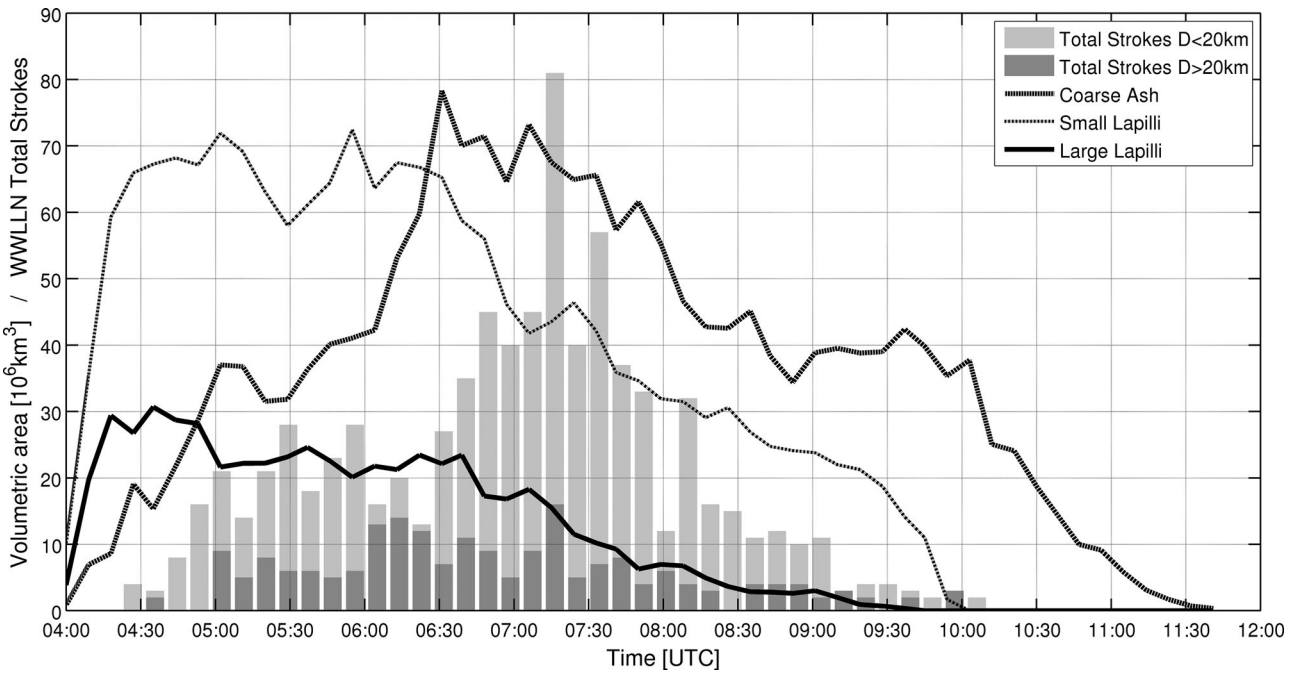

Fig. 9. Time evolution of the volumetric area of CA, SL, and LL classes, and WWLLN total strokes (bars) located less than 20 km from the volcano (light gray), and greater than 20 km (dark gray).

from 0.75 to 0.9 in the plume core, with Z_{DR} values between –1 to 0 dB are likely related to the coarse ash vertically oriented particles. In other hand, in the downwind ash cloud, horizontal reflectivity values range from 0 to 10 dBZ, ρ_{HV} is close to 1, and Z_{DR} ranging from –1 to 0 dB are observed close to 15 km AMSL. The particles in the downwind ash cloud are likely uniform, and are likely lower concentrations of nearly randomly oriented particles, or slightly vertically oriented particles.

C. Estimation of Volcanic Particle Classes

Fig. 7 shows the PPI at 5° of the predominant volcanic particle classes at three different times. The spatial distribution of volcanic classes strongly resembles the configuration of Z_{HH}. This effect is clearly expected from the classification method proposed associated with a single variable threshold. At the onset of the second pulse (04:00 UTC), the prevailing identified class is the LL with PO close to main core of the eruption, and

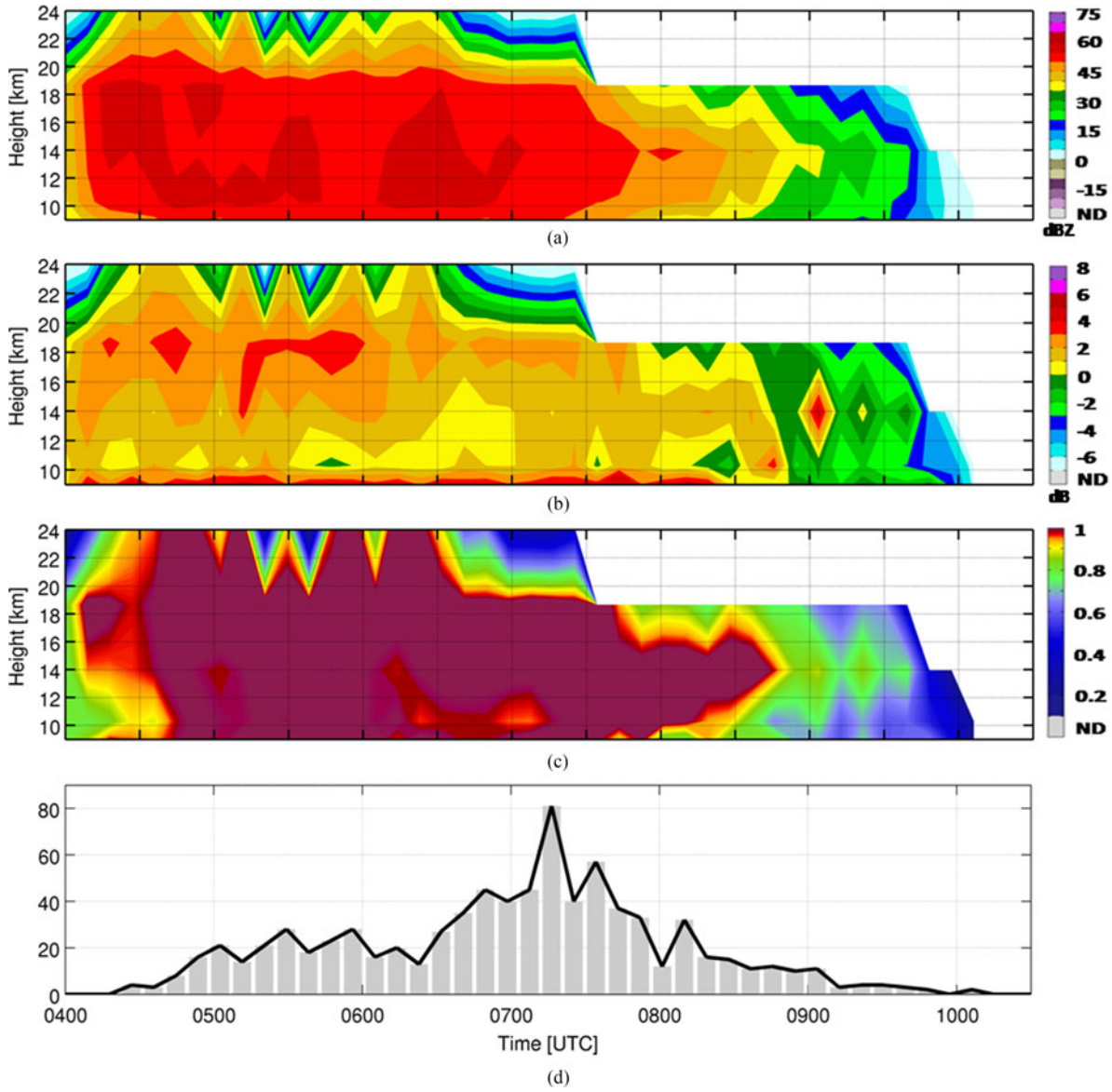

Fig. 10. Time evolution of a vertical reconstructed range-height indicator (RHI) profile of radar observables (Z_{HH}, Z_{DR}, and ρ_{HV}) calculated from the PPI data on vertical Calbuco vent, and WWLLN total strokes (bars) located less than 20 km from the volcano. (a) Horizontal Reflectivity. (b) Differential Reflectivity. (c) Correlation Coefficent. (d) WWLLN total strokes (D $<$ 20 km).

surrounded area of SL. At 04:18 UTC, the LL and SL classes range, particularly the latter begins to elongate toward the NNE, while CA class appears associated with the development of the volcanic plume advected by the predominant wind [27]. At 07:06 UTC, the plume well developed dominated by CA class orientation PO closer to the volcano and OO toward the edges is observed.

The area dominated by the LL and SL class does not seem to vary greatly. Similar results were shown by [5], at Mount Etna eruption using VARR-PX algorithm for a X-band frequency. The proposed threshold-based method can lead to inadequate classification results, because the radar observations for different particles and precipitation types are not mutually exclusive, but it is adequate for the interpretation of different classes of tephra and its separation.

V. Radar Observations and Lightning Activity

The total number of strokes detected by the WWLLN network related with the second pulse were 1016 strokes. Fig. 8(a) shows the spatial distribution of the total flash rate: most of them (>80%) were located in a range closer than 20 km to the vent, and associated with the main eruption column where COLMAX values exceed 35 dBZ [see Fig. 8(b)]. Interestingly, a similar reflectivity threshold has been found for lightning in thunderstorms [40]. A similar result were found in [33], where Lay *et al.* analyzed lightning activity generated by the eruption of the Cordón Caulle volcanic complex in June 2011. Additionally, the observed spatial distribution of lightning is collocated with the main eruption column and the volcanic ash plume generated by the eruption. It has been shown that high energy eruptions

can produce an effective plume electrification process within the eruption column [25], [26].

Note that we are assuming the predomanance of tephra particle within the plume. The presence of an ice cap over the eruption column is a debated issue (e.g., [16], [46]). Even thermal infrared brightness temperature difference (BTD) satellite-based techniques are almost useless due to the presence of bigger particles causing BTD saturation [46]. This implies that it is difficult to access and characterize the ice presence within the plume even using spaceborne measurements. A reasonable conjecture is that ice may contribute to nucleation of tephra particles in the plume layers above the freezing level thus modifying the particle density, but less affecting their microwave reflectivity which is dominated by denser silicate constituents and particle skin film [18]. On the other hand, smaller pure ice crystals are poorly detected at C-band so that their presence is only slightly influencing the radar backscaterring.

In order to analyze the time evolution of the lightning activity, Fig. 9 shows the total number of strokes, divided in two groups: strokes that occurred within a distance of 20 km to the vent and the ones located to a larger distance of 20 km, and the total volume of radar pixels divided in classification particles (CA, SL, and LL) without considering the orientation, as a function of the ground radar acquisition time. In contrary with the findings of [26], in this case the electrical activity begins to be detected by WWLLN roughly half an hour after the eruption started (at 04:00 UTC according to official reports SERNAGEOMIN and radar observations). This difference may be due to factors related to the detection efficiency of the network tends to detect the intense lightning strikes [33], [34] or the plume electrification processes became more efficient after a period of time [24].

After 06:30 UTC, close to the volcano (<20 km range), electrical activity shows a substantial increase before it reaches the maximum at approximately 07:20 UTC with more than 80 flashes in 9 min (rate $\sim$ 9 flashes/min). This behavior precedes a surge in the volume area of the CA and SL categories between 06:00 and 06:30 UTC. The latter occurs after a minimum in the area observed at 05:30 UTC, which could indicate an intensification of volcanic activity and a new injection of volcanic material into the atmosphere in the region of SL. Previous studies have linked an increase in lightning rates to the expanding size of the cloud observed by satellites [42], [43]. However, Van Eaton *et al*. in [27] suggested that the lightning was triggered by a pyroclastic density currents (PDCs) from Calbuco volcano, from the low-level ash clouds produced by the PDCs that introduced a new atmospheric charge layer capable of triggering cloud-to-ground lightning. This conclusion is related with the cessation of the upwind plume expansion sometime between 05:38 and 06:38 UTC, despite an ongoing eruption as shown the evolution of the CA volumetric area (see Fig. 9). After reaching the maximum in lightning activity, it begins to decrease until the network detects the last flashes at 10:00 UTC. This time coincides with the reduction of large particles (SL and LL) in the eruptive column.

Fig. 10 shows the time evolution of a vertical reconstructed range-height indicator (RHI) profile of radar variables (Z_{HH}, $\mathrm{Z_{DR}}$, and ρ_{HV}) calculated from the PPI data on vertical Calbuco vent in order to analyze in more detail the behavior of polarimetric variables in the main column of the eruption. As mentioned above, the cross section shows the presence of large particles ($\mathrm{Z_{HH}} > 55$ dBZ) between 10 and 12 km AMSL, with a wide variety of particle shapes (CA, SL, and LL) and sizes ($\rho\mathrm{HV} < 0.95$). This behavior is principally denoted between 06:10 UTC and the peak of electrical activity close to 07:20 UTC. Minimum values of ZDR (lower than 1 dB) are observed in this region denoting the vertical orientation of the particles due to a possible presence of electric field. It is important to remark the showed values are an average of the whole main column over the volcano (eight pixels in range direction). This average smoothed the values of the variables showed in Fig. 10. This result is consistent with the findings of [25] in a study of a comprehensive global database of volcanic lightning. In that study, it is shown that eruptions with ash plume heights of 7 to 13 km AMSL, are more efficient compared with eruptions of lesser heights. Also, James *et al*. [44] suggested that the dependency of charge separation efficiency with particle size may act as a secondary process of capturing ions, which is both a function of particle size and falling speed.

VI. Conclusions

The eruption of Calbuco volcano on April 22–23, 2015 was the first major volcanic eruption observed by polarimetric weather radar in South America providing a unique example of dual-polarization radar observations worldwide. C-band dual polarization radar data can clearly detect the volcanic plume and the ash cloud spreading in the surrounding area of the Calbuco volcano which showed a horizontal extension of approximately 100×160 km in PPI images of horizontally polarized reflectivity.

Dual-polarization signatures of C-band RMA0 radar data show a sensitivity to particle concentration, type, orientation, and composition during the evolution of the plume. Z_{HH} shows values greater than 50 dBZ within the eruption plume core and values between 5 and 15 dBZ away from it associated with the ash drifting plume in upper levels. ρ_{HV} shows a dramatic decrease in the area intersected by the core of the main column of the eruption, this effect is related to the diversity of shapes and sizes of large particles (e.g., large lapilli). This might be interpreted as a consequence of turbulent effects that facilitate the shuffling of various tephra particles causing the decrease of ρ_{HV} [2]. Z_{DR} is strongly affected, more than other radar variables, by factors depending on the radar system (calibration bias) and the electromagnetic scattering within the plume character itself (particle orientation effects induced by the electric field and/or strong turbulence), but some evidences of the orientation is observed, denoting a PO close to main core of the eruption.

The total number of strokes detected by the WWLLN network related with the second pulse were 1016 strokes, the spatial distribution of the strokes are located close to the vent (<20 km) and the initiation of the lightning activity is delayed half an hour from the initiation of the second eruption. Highest lightning rate close to the vent is associated with an increase of CA volumetric

rate that can be related with an increase in the eruption energy. Additionally, the "umbrella cloud" method based on satellite images in order to estimate the mass eruption rate [45] can be reformulated using the CA volumetric rate as a new input more adequate than GOES infrared images. Even thermal infrared brightness temperature difference (BTD) satellite-based techniques are useless due to the presence of bigger particles causing BTD saturation. The latter implies that it is impossible from satellite or radar to discriminate between a water and a tephra (i.e., ash) cloud. Our conjecture is that ice may contribute to nucleation of tephra particles thus modifying the particle density more than its reflectivity due to skin effects.

This case study provides an excellent example that C-band dual-polarization radar system can provide an emerging scientific requirement to differentiate between CA, SL, and LL categories during a volcanic eruption providing information to aviation forecasts and emergency managers. Future work has to be made in order to include ρ_{HV} and K_{DP} in order to have a better discrimination of classes. Major future challenges are concentrated in the validation of these classification techniques, and further analysis must to be done using multiple remote sensing evaluation to evaluate between different particle types. The synergy between ground-based weather radars, satellite products from multisensor systems, lightning activity, and other remote or local sensors, is a major future challenge in order to constrain the initial parameters associated to the density and location of the different particles to improve the performance of ash dispersion forecast models.

ACKNOWLEDGMENT

Authors would like to thank the Editor who handled this paper and the three anonymous reviewers for providing truly outstanding comments and suggestions that significantly helped them in improving the manuscript. They also would like to thanks G. Cabrera, F. Renolfi, and I. Landerreche from INVAP S.E for control radar observations during the volcano eruption and productive discussions, and World Wide Lightning Location Network for providing the lightning data used in this paper. S. W. Nesbitt would like to thank to CONICET sabbatical visiting fellowship and Argentina—National Meteorological Service for support his sabbatical visit to Argentina.

REFERENCES

[1] R. D. Cadle *et al.*, "Atmospheric implications of studies of Central American volcanic eruption clouds," *J. Geophys. Res.*, vol. 84, pp. 6961–6968, 1979.

[2] M. Montopoli, G. Vulpiani, D. Cimini, E. Picciotti, and F. S. Marzano, "Interpretation of observed microwave signatures from ground dual polarization radar and space multi-frequency radiometer for the 2011 Grímsvötn volcanic eruption," *Atmos. Meas. Techn.*, vol. 7, no. 2, pp. 537–552, Feb. 2014.

[3] L. G. Mastin, M. Guffanti, J. E. Ewert, and J. Spiegel, "Preliminary spreadsheet of eruption source parameters for volcanoes of the world: US geological survey open-file report 2009-1133," version 1.2, p. 25, [Online]. Available: http://pubs.usgs.gov/of/2009/1133/, 2009.

[4] F. S. Marzano, M. Lamantea, M. Montopoli, S. Di Fabio, and E. Picciotti, "The eyjafjöll explosive volcanic eruption from a microwave weather radar perspective," *Atmos. Chem. Phys.*, vol. 11, pp. 9503–9518, 2011.

[5] G. Vulpiani, M. Montopoli, E. Picciotti, and F. S. Marzano, "On the use of polarimetric X-band weather radar for volcanic ash clouds monitoring," in *Proc. AMS Radar Conf.*, Pittsburgh, PA, USA, 2011.

[6] P. Arason, G. N. Petersen, and H. Bjornsson, "Plume-top altitude time-series during 2010 volcanic eruption of Eyjafjallajökull," *Earth Syst. Sci. Data Discuss.*, vol. 4, pp. 1–25, May 2011.

[7] M. Maki *et al.*, "Quantitative volcanic ash estimation by operational polarimetric weather radar," in *Proc. 9th Int. Symp. Tropospheric Profiling*, L'Aquila, Italy, 2012, p. 5.

[8] P. W. Webley and L. G. Mastin, "Improved prediction and tracking of volcanic ash clouds," *Special Issue Volcanic Ash Clouds, Volcanol. Geoth. Res.*, vol. 186, pp. 1–9, 2009.

[9] K. H. Wohletz, M. F. Sheridan, and W. K. Brown, "Particle size distributions and the sequential fragmentation/transport theory applied to volcanic ash," *J. Geophys. Res.*, vol. 94, no. B11, pp. 15703–15721, 1989.

[10] R. S. J. Sparks *et al.*, *Volcanic Plumes*. Hoboken, NJ, USA: Wiley, p. 574, 1997.

[11] F. S. Marzano, E. Picciotti, M. Montopoli, and G. Vulpiani, "Inside volcanic clouds: Remote sensing of ash plumes using microwave weather radars," *Bull. Am. Meteor. Soc.*, vol. 94, pp. 1567–1586, Oct. 2013.

[12] F. S. Marzano, E. Picciotti, G. Vulpiani, and M. Montopoli, "Synthetic signatures of volcanic ash cloud particles from X-band dual-polarization radar," *IEEE Trans. Geosc. Remote Sens.*, vol. 50, no. 1, pp. 193–211, Jan. 2012.

[13] D. M. Harris and W. I. Rose, Jr., "Estimating particle sizes, concentrations, and total mass of ash in volcanic clouds using weather radar," *J. Geophys. Res.*, vol. 88, no. C15, pp. 10 969–10 983, 1989.

[14] C. Lacasse, S. Karlsdottir, G. Larsen, H. Soosalu, W. I. Rose, and G. G. J. Ernst, "Weather radar observations of the Hekla 2000 eruption cloud, Iceland," *Bull. Volcanol.*, vol. 66, pp. 457–473, 2004.

[15] F. S. Marzano, S. Barbieri, G. Vulpiani, and W. I. Rose, "Volcanic ash cloud retrieval by ground-based microwave weather radar," *IEEE Trans. Geosci. Remote Sens.*, vol. 44, no. 11, pp. 3235–3246, Nov. 2006.

[16] F. S. Marzano, S. Barbieri, E. Picciotti, and S. Karlsdóttir, "Monitoring subglacial volcanic eruption using C-band radar imagery," *IEEE Trans. Geosci. Remote Sens.*, vol. 48, no. 1, pp. 403–414, Jan. 2010.

[17] F. S. Marzano, G. Vulpiani, and W. I. Rose, "Microphysical characterization of microwave radar reflectivity due to volcanic ash clouds," *IEEE Trans. Geosci. Remote Sens.*, vol. 44, no. 2, pp. 313–327, Feb. 2006.

[18] F. S. Marzano, S. Marchiotto, C. Textor, and D. Schneider, "Model-based weather radar remote sensing of explosive volcanic ash eruption," *IEEE Trans. Geosci. Remote Sens.*, vol. 48, no. 10, pp. 3591–3607, Oct. 2010.

[19] J. F. Crouch, N. Pardo, and C. A. Miller, "Dual polarisation C-band weather radar imagery of the 6 august 2012 Te Maari eruption, Mount Tongariro, New Zealand," *J. Volcanol. Geothermal Res.*, vol. 286, pp. 415–436, Oct. 2014.

[20] R. J. Thomas *et al.*, "Electrical activity during the 2006 Mount St. Augustine volcanic eruptions," *Science*, vol. 315, 2007, Art. no. 1097.

[21] R. J. Thomas *et al.*, "Lightning and electrical activity during the eruptions of Augustine volcano," in *The 2006 Eruption of Augustine Volcano, Alaska: U.S. Geological Survey Professional Paper*, 1769–1725, pp. 579–608, 2010.

[22] A. J. Bennett, P. Odams, D. Edwars, and P. Arason, "Monitoring of lightning from the April-May 2010 Eyjafjallajökull volcanic eruption using a very low frequency lightning location network," *Environ. Res. Lett.*, vol. 5, 2010, Art. no. 044013.

[23] R. G. Harrison, K. A. Nicoll, Z. Ulanowski, and T. A. Mather, "Self-charging of the Eyjafjallajökull volcanic ash plume," *Environ. Res. Lett.*, vol. 5, 2010, Art. no. 024004.

[24] S. A. Behnke *et al.*, "Observations of volcanic lightning during the 2009 eruption of redoubt volcano," *J. Volcanol. Geothermal Res.*, vol. 259, pp. 214–234, 2013.

[25] S. R. McNutt and E. R. Williams, "Volcanic lightning: Global observations and constraints on source mechanisms," *Bull. Vulcanol.*, vol. 72, pp. 1153–1167, Aug. 2010.

[26] M. G. Nicora, R. E. Bürgesser, A. Rosales, E. J. Quel, and E. E. Avila, "Actividad eléctrica asociada a la erupción del complejo volcánico Cordón Caulle durante 2011," *Meteorológica*, vol. 38, no. 2, pp. 121–131, 2013.

[27] A. R. Van Eaton *et al.*, "Volcanic lightning and plume behavior reveal evolving hazards during the April 2015 eruption of Calbuco volcano, Chile," *Geophys. Res. Lett.*, vol. 43, pp. 3563–3571, 2016.

[28] M. E. Petit-Breuilh, "Cronología Eruptiva Histórica de los volcanes Osorno y Calbuco," *Servicio Nacional de Geología y Minería*, Boletín No. 53, p. 45, Santiago, Chile, 1999.

[29] J. Clavero, E. Godoy, G. Arancibia, C. Rojas, and H. Moreno, "Multiple Holocene sector collapses at Calbuco volcano, Southern Andes," *IAVCEI General Assembly,* Reykjavik, Iceland, 2008, p. 41.
[30] A. Castruccio and J. Clavero, "Lahar simulation at active volcanoes of the Southern Andes: Implications for hazard assessment," *Natural Hazards*, vol. 7, no. 2, pp. 693–716, 2015.
[31] A. Segura *et al.*, "Fallout deposits of the 22-23 April 2015 eruption of Calbuco volcano, Southern Andes," in *Proc. XIV Congreso Geológico Chileno*, La Serena, Chile, 2015, pp. 182–185.
[32] *Radar for Meteorologists*, 4th ed. Columbia, MO, USA: Rinehart Publications, 2004, p. 66.
[33] E. H. Lay, R. H. Holzworth, C. J. Rodger, J. N. Thomas, O. Pinto, Jr., and R. L. Dowden, "WWLL global lightning detection system: Regional validation study in Brazil," *Geophys. Res. Lett.*, vol. 31, 2004, Art. no. L03102.
[34] R. L. Dowden, J. B. Brundell, and C. J. Rodger, "VLF lightning location by time of group arrival (TOGA) at multiple sites," *J. Atmos. Sol-Terr. Phy.*, vol. 64, pp. 817–30, 2002.
[35] M. L. Hutchins, R. H. Holzworth, J. B. Brundell, and C. J. Rodger, "Relative detection efficiency of the world wide lightning location network," *Radio Sci.*, vol. 47, no. 6, pp. 1–9, 2012.
[36] S. F. Abarca, K. L. Corbosiero, and T. J. Galarneau, "An evaluation of the Worldwide Lightning Location Network (WWLLN) using the National Lightning Detection Network (NLDN) as ground truth," *J. Geophys. Res.*, vol. 115, no. D18, pp. 1–11, 2010.
[37] W. I. Rose, A. B. Kostinski, and L. Kelley, "Real-time C band radar observations of 1992 eruption clouds from Crater Peak vent, Mount Spurr volcano, Alaska," *U.S. Geol. Surv. Bull.*, vol. 2139, pp. 19–26, 1995.
[38] F. S. Marzano, S. Barbieri, G. Vulpiani, and W. I. Rose, "Volcanic ash cloud retrieval by ground-based microwave weather radar," *IEEE Trans. Geosci. Remote Sens.*, vol. 44, no. 11, pp. 3235–3246, Nov. 2006.
[39] C. M. Riley, W. I. Rose, and G. J. S. Bluth, "Quantitative shape measurements of distal volcanic ash," *J. Geophys. Res.*, vol. 108, no. B10, 2003, Art. no. 2504.
[40] D. S. Zrnić, G. Zhang, V. Melnikov, and J. Andrić, "Three-body scattering and hail size," *J. Appl. Meteor. Climatol.*, vol. 49, pp. 687–700, 2010.
[41] S. Astudillo, L. Bertin, and D. Bertin, "Características texturales y composicionales de la tefra del ciclo eruptivo de abril-mayo de 2015 del volcán Calbuco," in *Proc. XIV Congreso Geológico Chileno*, La Serena, Chile, 2015.
[42] E. R. Williams, "Large-scale charge separation in thunderclouds," *J. Geophys. Res.*, vol. 90, pp. 6013–6025, 1985.
[43] S. A. Behnke and E. C. Bruning, "Changes to the turbulent kinematics of a volcanic plume inferred from lightning data," *Geophys. Res. Lett.*, vol. 42, pp. 4232–4239, 2015.
[44] M. R. James, S. J. Lane, and J. S. Gilbert, "Volcanic plume electrification: Experimental investigation of a fracture-charging mechanism," *J. Geophys. Res.*, vol. 105, pp. 16641–16649, 2000.
[45] R. S. J. Sparks, "The dimensions and dynamics of volcanic eruption columns," *Bull. Volcanol.*, vol. 48, pp. 3–15, 1986.
[46] W. I. Rose, G. J. S. Bluth, and G. G. J. Ernst, "Integrating retrievals of volcanic cloud characteristics from satellite remote sensors: A summary," *Philos, Trans. Roy. Soc. London*, vol. A358, pp. 1538–1606, 2000.

Luciano Vidal received the Master's degree in atmospheric sciences from the University of Buenos Aires, City of Buenos Aires, Argentina, in 2009. He received the Ph.D. degree in meteorology with the focus in mesoscale convective system studies in Argentina using different remote sensing sources in 2014.

In 2011, he was with the Department of Atmospheric Sciences, The University of Utah, Salt Lake City, USA, where he was an Assistant Researcher at the TRMM PMM Science Group. Since April 2014, he has been with the National Meteorological Service, Buenos Aires, Argentina, where he is Principal Researcher in weather radar and meteorological satellite. Since December 2015, he has been the Director of the Project PIDDEF 05/14 "Monitoring thunderstorms with weather radars in Argentina."

Stephen W. Nesbitt received the B.S. degree in meteorology (*summa cum laude*) from the State University of New York at Oswego, Oswego, NY, USA, in 1997, the M.S. degree in meteorology from Texas A&M University, College Station, TX, USA, in 1999, and the Ph.D. degree in meteorology from the University of Utah, Salt Lake City, UT, USA, in 2003.

He was a Research Scientist in the Department of Atmospheric Science, Colorado State University from 2003 to 2006. He joined the faculty in Urbana in 2006. His research and teaching interests reside in the remote sensing of precipitation using radar and passive microwave sensors, mesoscale and cloud dynamics and microphysics, land-atmosphere interaction, and numerical simulation, data science, and high-performance computation. He is a member of the NASA Precipitation Measurement Missions Science Team and the NASA Ocean Vector Winds Science Team, and is heavily involved in research involving NASA's Tropical Rainfall Measurement Mission and Global Precipitation Measurement satellite missions.

Paola Salio received the Master's and Ph.D. degree in atmospheric science from the University of Buenos Aires, Buenos Aires, Argentina, in 1997 and 2002, respectively.

In 1993, she joined the Department of Atmospheric and Oceanographic Science, University of Buenos Aires, as a Teaching Assistant, and she became an Assistant Professor in 2004. Since March 2004, she has been a member of National Research and Technology Council as a Researcher. Her current research interests include mesoscale meteorology, synoptic meteorology, radar meteorology, and meteorological satellite applications.

Dr. Salio is a member of IAMAS Scientific Member Committee, Hight Impact Weather—WMO Project, member of the Scientific Group representation from Argentina GPM-Global Precipitation Measurement, and steering group of RELAMPAGO field experiment. She was awarded by World Meteorological Organization, Young Research Prize for her paper entitled: "Mesoscale Convective Systems over Southeastern South America and its relationship with the South American Low Level Jet."

Camila Farias received the Master's degree in geophysics from the University of La Plata, Buenos Aires, Argentina, in 2013. She is currently working toward the Ph.D. degree in geophysics on volcanoes infrasound techniques.

Since August 2013, she has been Geophysics Research at National Meteorological Service, Buenos Aires, Argentina. Her main research interests include the design and development of a database containing the eruptive history of active volcanoes in the Southern South America. She focuses on the assessment of volcanic explosivity parameters to adjust the initialization of the ash dispersion model, in support of the aviation and civil defense.

María Gabriela Nicora received the Ph.D. degree in geophysics with specialization in lightning activity, from the Universidad Nacional de La Plata, La Plata, Argentina, in 2014.

Since 2010, she has been with the Institute of scientific and technical research for defense (CITEDEF - Ministerio de Defensa) and has been the Chief Project Manager of Lightning Research since 2014. She has mapped lightning activity over South America based on ground antennas, and characterized the diurnal cycle of lightning based upon satellite data, also she has been involved with the lightning activity from volcanic eruptions.

María Soledad Osores received the Master's degree in atmospheric sciences from the University of Buenos Aires, Buenos Aires, Argentina, in 2012. Since 2012, she has been working toward the Ph.D. degree on uncertainty quantification of ash dispersion numerical model input parameters and ash dispersion ensemble forecasting.

She is working in joint collaboration with researchers from the Barcelona Super computing Center, Centre of Investigations of the Sea and Atmosphere, the National Scientific and Technical Research Council, the National Space Activities Commission, Naval Hydrographic Service and the National Meteorological Service of Argentina. Since 2010, as a member of the PIDDEF 41/10 project directed by Dr. E. Collini, she started working at National Meteorological Service specializing on ash dispersion modeling. Since that moment she offers technical support to Buenos Aires Volcanic Ash Advisory Center.

Luigi Mereu received the M.Sc. degree in telecommunication engineering and the Ph.D. in remote sensing from the Sapienza University of Rome, Rome, Italy, in 2012 and 2016, respectively.

In 2012, he joined the Department of Information Engineering, Sapienza University of Rome, Italy, and the Centre of Excellence CETEMPS in L'Aquila to cooperate on radar remote sensing of volcanic ash clouds within the ICT Ph.D. program. He is involved within the FUTUREVOLC and APHORISM European projects started in 2012 and 2014, respectively.

Dr. Mereu received the IEEE GRS South Italy Award for the Best Master Thesis in remote sensing in 2012.

Frank S. Marzano (S'89–M'99–SM'03–F'15) received the Laurea degree (*cum laude*) in electrical engineering and the Ph.D. degree in applied electromagnetics both from the Sapienza University of Rome, Italy, 1988 and 1993, respectively.

In 1992, he was a Visiting Scientist at Florida State University, Tallahassee, FL, USA. After being a Lecturer at the University of Perugia, Italy, in 1997, he joined the Department of Electrical Engineering, University of L'Aquila, Italy teaching courses on electromagnetic fields. In 1999, he was at Naval Research Laboratory, Monterey, CA, USA, as a Visiting Scientist. In 2002, he co-founded Center of Excellence on Remote Sensing and Forecast Modeling (CETEMPS), L'Aquila. In 2005, he finally joined the Department of Information engineering, Electronics and Telecommunications, Sapienza University of Rome, Italy, where he presently teaches courses on antennas, propagation, and remote sensing. Since 2007, he has been the Vice Director of CETEMPS of the University of L'Aquila, Italy, where he became the Director in 2013. His current research concerns passive and active remote sensing of the atmosphere from ground-based, airborne, and space-borne platforms and electromagnetic propagation studies. He has published more than 130 papers on refereed International Journals, more than 30 contributions to international Book chapters and more than 260 extended abstract on international and national congress proceedings.

Dr. Marzano has been the Associate Editor of IEEE Geoscience Remote Sensing Letters since 2004. Since January 2011, he has been the Associate Editor of the journal EGU Atmospheric Measurements Techniques. He is a Fellow of the Royal Meteorological Society as well as member of the MWI-ICI Science Advisory Group of EuMetSat and PMM Science Team of NASA.